FTIR Studies of the Reaction of Gaseous NO with HNO_3 on Porous Glass: Implications for Conversion of HNO_3 to Photochemically Active NO_x in the Atmosphere

Michihiro Mochida[†] and Barbara J. Finlayson-Pitts*

Department of Chemistry, University of California—Irvine, Irvine, California 92697-2025

Received: April 18, 2000; In Final Form: July 20, 2000

The heterogeneous reaction of HNO_3 adsorbed on porous glass surfaces with gaseous NO was investigated using transmission Fourier transform infrared (FTIR) spectroscopy at room temperature. The amount of adsorbed HNO_3 varied from $(4.2-110) \times 10^{17}$ molecules of HNO_3 on a 6 cm^2 porous glass plate whose BET surface area was measured to be 28.5 ± 0.6 m^2 (2σ). The initial concentration of gaseous NO varied from $(0.2-6) \times 10^{17}$ molecules cm^{-3}. A rapid release of NO_2 into the gas phase was observed to occur simultaneously with a decrease in adsorbed HNO_3. A trace amount of gaseous HONO was also formed. The measured yields of NO_2 and loss of HNO_3 and NO are consistent with the net reaction $2HNO_3 + NO \rightarrow 3NO_2 + H_2O$ which is due to $HNO_3 + NO \rightarrow HONO + NO_2$, followed by $HONO + HNO_3 \rightarrow 2NO_2 + H_2O$ and/or $2 \times (HNO_3 + NO \rightarrow HONO + NO_2)$ followed by $2HONO \rightarrow NO + NO_2 + H_2O$. Both $^{15}NO_2$ and $^{14}NO_2$ were observed as reaction products when ^{15}NO and $^{14}HNO_3$ were used as the reagent species, indicating that some of the NO_2 produced originates in HNO_3. The measured decay rates for adsorbed HNO_3 were first order in NO. The rates initially increase with increasing HNO_3 but tend to plateau, consistent with complete surface coverage and the formation of multilayers of HNO_3, perhaps in part in the pores. Extrapolation of these results to atmospheric NO levels suggests that this heterogeneous reaction may serve as a mechanism to regenerate photochemically active forms of NO_x and nitrous acid from HNO_3 in the atmosphere.

Introduction

Nitric acid is present throughout the atmosphere both in the gas and aqueous phases. HNO_3 is believed to be an end product of oxidation processes of nitrogen oxides in the atmosphere. Removal processes include reaction with OH and NH_3 (reversible) and photolysis, as well as wet and dry deposition which tend to predominate in the lower troposphere.[1] A number of researchers have suggested pathways whereby HNO_3 is reduced in the atmosphere, yielding photochemically active forms of NO_x.[1] For example, Chatfield[2] hypothesized that the discrepancy between the measured ratio of $[HNO_3]/[NO_x] \sim 5$ in the free troposphere and the values of 15−100 predicted by model calculations could be due to liquid-phase reactions of HCHO with HNO_3 in aerosols and cloud droplets. The conversion of HNO_3 into NO has been reported to proceed heterogeneously on soot surfaces at room temperature (e.g. Rogaski et al.[3]), although at lower HNO_3 concentrations and temperatures, only physical adsorption may occur.[4] Some model studies have suggested that if this reduction on soot occurs in the atmosphere, it could bring the measurements and models into better agreement.[5,6]

Photochemical conversion of HNO_3 to NO_x was also suggested by recent measurements of NO_y in snowpacks.[7,8] Honrath and co-workers hypothesized that this is due to the photolysis of nitrate[9−11] on the ice, analogous to the photolysis of nitrate ions in the aqueous phase:

$$NO_3^- + h\nu\ (300-350\ nm) \rightarrow NO_2 + O^- \quad (1a)$$

$$\rightarrow NO_2^- + O \quad (1b)$$

$$O^- + H_2O \rightarrow OH + OH^- \quad (2)$$

In gas-phase kinetics studies, two nonphotochemical reduction pathways for HNO_3 have been reported, the reaction 3 with NO[12−15] and reaction 4 with nitrous acid:[14−17]

$$HNO_3(g) + NO(g) \rightarrow HONO(g) + NO_2(g)$$
$$\Delta H^\circ = -1.4\ kJ\ mol^{-1}, \quad \Delta G^\circ = -6.5\ kJ\ mol^{-1} \quad (3)$$

$$HNO_3(g) + HONO(g) \rightarrow 2\ NO_2(g) + H_2O(g)$$
$$\Delta H^\circ = +39.2\ kJ\ mol^{-1}, \quad \Delta G^\circ = -5.3\ kJ\ mol^{-1} \quad (4)$$

The upper limits for these rate constants, $k_3 < 3.4 \times 10^{-22}$ cm^3 $molecule^{-1}$ s^{-1} [15] and $k_4 < 7 \times 10^{-19}$ cm^3 $molecule^{-1}$ s^{-1},[17] imply these reactions are not important in the atmosphere, although there appeared to also be some contribution from heterogeneous reactions on the walls of the reaction chamber. A heterogeneous reaction of NO with HNO_3 was suggested by Besemer and Nieboer as a source of HONO to explain the concentration−time profiles of major species generated in smog chamber studies of mixtures of NO_x with CO and propane.[18] In addition, reaction 3 has been proposed, based on consideration of the thermodynamics, as potentially occurring heterogeneously under some atmospheric conditions.[19]

However, to the best of our knowledge, there has been no systematic study of the *heterogeneous* reactions of HNO_3 with

* To whom correspondence should be addressed. E-mail: bjfinlay@uci.edu. Phone: (949) 824−7670. FAX: (949) 824−3168.

[†] Now at Institute of Low-Temperature Science, Hokkaido University, N19 W8, Kita-ku, Sapporo 060-0819, Japan.

10.1021/jp001471a CCC: $19.00
Published on Web 10/10/2000

gas-phase nitrogen compounds. A major reason may be the difficulty in measuring both surface adsorbed and gas-phase species simultaneously.

In the work reported here, the heterogeneous reaction of surface-adsorbed HNO_3 with gaseous NO on porous glass (silica) surfaces was investigated using transmission FTIR spectroscopy. Porous glass was used primarily as a means of holding adsorbed water and HNO_3 in such a manner that transmission FTIR could be used to readily follow species on the surface; however, given that silica is a major component of dust particles derived from crustal materials,[1] these studies are also relevant to reactions of HNO_3 on dust particles in the atmosphere. Both gas and surface-adsorbed species were identified from their infrared absorption bands and followed as a function of time. Isotopically labeled ^{15}NO was also used in some experiments to investigate the source of nitrogen atoms in the NO_2 product. We show that the heterogeneous reaction of HNO_3 with NO on silica surfaces proceeds significantly faster than in the gas phase, as suggested by observations in earlier gas-phase studies.[12−15] This reaction is shown to be a potentially important reduction process for HNO_3 back to NO_x as well as a source of HONO in the atmosphere.

Experimental Section

The experimental apparatus, described in detail elsewhere,[20] consisted of an FTIR spectrometer (Mattson Research Series) and a borosilicate glass reaction cell of volume 79 cm^3 and path length 6.7 cm. A 6 cm^2 porous glass plate (Vycor, Corning), with surface area 28.5 ± 0.6 m^2 (2σ) measured by the Brunauer−Emmett−Teller (BET) method using nitrogen as the adsorbate (ASAP 2000, Micromeritics), could be moved in and out of the infrared beam. Since silica has strong infrared absorptions[21] below 2000 cm^{-1} where those of interest due to nitrogen oxides also exist, the porous glass plate must be as thin as possible. A commercially available porous glass plate (20 mm × 30 mm × 1 mm) was etched using 7.7 (v:v) % HF solution for 21 min after masking the edge of the plate. A porous glass plate with a center area of ∼3 cm^2 as thin as 0.1 mm was obtained. Between independent experiments, the porous glass was cleaned by soaking in water (Barnstead, Nanopure, 18 MΩ cm) to remove adsorbed species such as nitric acid.

Silica surfaces are terminated by hydroxyl groups (Si−OH) which hold water molecules via hydrogen bonding. There are three types of surface species:[21] (i) free vibrating hydroxyl groups, (ii) hydrogen bonded hydroxyl groups, and (iii) strained siloxane bridges. Their relative abundances depend on the heat treatment of the silica surface and the H_2O partial pressure. Under most of our experimental conditions where the porous glass was not heated, hydroxyl groups terminate the silica surface and act to hold water on the surface.

The porous glass was placed in the cell and evacuated for 3−10 h. The porous glass was exposed to $10^{16} - 10^{17}$ molecules cm^{-3} of gaseous HNO_3 for half an hour and then pumped out to remove gaseous and some adsorbed HNO_3. On rough pumping, a slow decrease in the peak intensity at 1677 cm^{-1} was observed due to desorption of surface HNO_3. To initiate the reaction with NO, the valve to the pump was closed and gaseous NO at concentrations from 2×10^{16} to 6×10^{17} molecules cm^{-3} was introduced. All the reactions were carried out at room-temperature either without added carrier gas or with ∼500 Torr of He added to the cell.

Concentrations of the gas-phase species NO, NO_2, HNO_3, and N_2O were obtained by measuring the intensities of the infrared bands centered at 1876, 1617, 1711, and 2224 cm^{-1}, respectively, compared to calibration spectra recorded for these gases under conditions of pressure and temperature used in these experiments. HONO was measured using its absorption at 1263 cm^{-1} and the integrated band intensity determined in previous studies in this laboratory.[22]

To quantify the amount of surface adsorbed HNO_3, and to calibrate its 1677 cm^{-1} infrared band, a certain amount of HNO_3 was adsorbed on the surface and the peak intensity at 1677 cm^{-1} was recorded. The porous glass plate was then removed from the cell and soaked in Nanopure water. The concentration of nitrate ion in solution was measured using ion chromatography (column, Vydac; mobile phase, potassium hydrogen phthalate 2×10^{-3} M; conductivity detector, Wescan). Since the inner walls of the reaction cell also adsorb HNO_3, these walls were rinsed with water and the solution was collected and analyzed. A comparison of these results show that >90% of the HNO_3 was adsorbed on the porous glass plate rather than on the inner cell walls, consistent with the high surface area of the porous glass relative to that of the reaction cell. The number of adsorbed HNO_3 molecules was varied from 4.2×10^{17} to 1.1×10^{19} molecules.

Single beam spectra were recorded with the porous glass either in the path of the infrared beam or withdrawn from the beam, as well as with and without the reactants in the cell. The ratio (S_{pg}/S_{pg}^0) of the single beam spectrum with the porous glass and reactant/product mixture in the beam (S_{pg}) to that without the reactants (S_{pg}^0) is used to obtain the absorbance due to gases plus surface-adsorbed species. This allows the strong silica absorptions-to-be ratioed out. Similarly, the ratio S_g/S_g^0 of the analogous single beam spectra with (S_g) and without (S_g^0) the reactants/products and with the porous glass withdrawn from the infrared beam was used to obtain the absorbance of the gases alone. Subtracting the spectrum of the gas species from that of the combined gas plus surface species gives the spectrum due to surface-adsorbed species alone. Infrared spectra were typically recorded at a resolution of 1 cm^{-1}, or for the kinetic studies, at 4 cm^{-1}. The number of scans was varied between 1 and 1024, depending on the S/N ratio and time resolution required for experiments.

Reagents. Nitric oxide used in the experiment (Matheson 99%) was passed through an acetone/dry ice bath trap at 195 K to remove impurities such as HNO_3. Nitrogen dioxide was synthesized by combining NO with excess oxygen (Oxygen Service Company, 99.993%) and then purified by condensing the mixture at 195 K and pumping away the excess O_2. NO_2 was stored in a glass bulb covered with a dark cloth to prevent photolysis in room lights. Gaseous nitric acid was obtained from the vapor above a 1:2 mixture of concentrated HNO_3 (69.3 wt % HNO_3, Fisher Chemical) and H_2SO_4 (95.7 wt %, Fisher Chemical). Nitrous oxide (99.99%, Liquid Carbonic) was also used for some experiments. He (Liquid Carbonic, 99.999%) was used as a buffer gas for some experiments.

Results and Discussion

A. Formation of NO_2 by Exposure of HNO_3 Adsorbed on Porous Glass to Gas-Phase NO. Figure 1a shows a spectrum of surface-adsorbed HNO_3. A peak that does not show significant rotational structure was observed at 1677 cm^{-1}, in agreement with previous studies by Grassian and co-workers[23] and Barney and Finlayson-Pitts.[20] A similar peak has been observed for undissociated nitric acid in water solutions.[24,25] The concentration of gas-phase HNO_3, measured using its 1711 cm^{-1} band, was small compared to the amount of surface adsorbed HNO_3. For instance, when the amount of surface

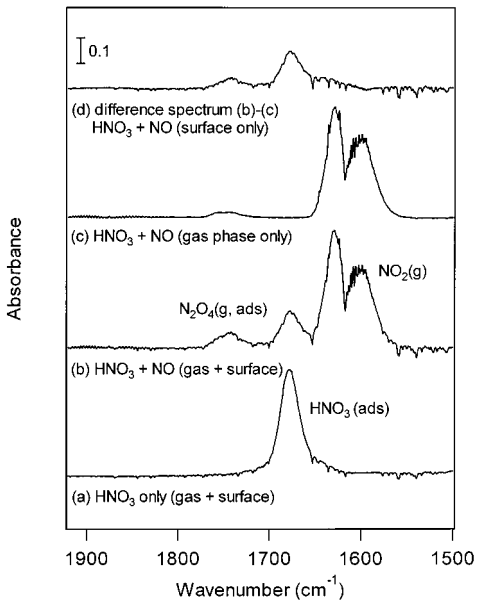

Figure 1. FTIR spectra of (a) surface species after the introduction of HNO_3; the porous glass has 9.4×10^{18} adsorbed molecules of HNO_3 (determined by ion chromatography), (b) spectrum of gas plus surface species 60 min after introduction of NO (6.7×10^{16} molecules cm^{-3}) along with 460 Torr of He to the reaction cell, (c) the gas-phase spectrum under the same conditions as (b), and (d) the difference spectrum between (b) and (c) due to surface adsorbed species. The absorbance scale is the same for all spectra.

adsorbed HNO_3 was 1×10^{19} molecules (based on measurements by ion chromatography), the gas-phase HNO_3 was 2.2×10^{15} molecules cm^{-3}, corresponding to a total of 1.7×10^{17} gas-phase HNO_3 in the cell.

Figure 1b−d show typical spectra from reaction of adsorbed HNO_3 with gaseous NO. Figure 1b is the spectrum of both gas and surface species after 60 min reaction time; the surface HNO_3 has decreased, while NO_2 and N_2O_4 have increased. Figure 1c is the gas phase spectrum which shows only NO_2 and small amounts of N_2O_4. Figure 1d is the difference spectrum (Figure 1d = 1b minus 1c) which shows only surface-adsorbed species. While essentially all of the NO_2 is in the gas phase, roughly half of the intensity of the N_2O_4 band around 1750 cm^{-1} is due to the surface-adsorbed species. The gas-phase NO is not consumed completely, and its steady-state concentration is ~25% of its initial value.

The initial conditions for a series of experiments designed to measure the changes in the gas and surface species are summarized in Table 1. The reaction stoichiometries between the initial concentrations and steady state are also summarized.

Small amounts of HONO were also formed in the gas phase. As shown in Figure 2, the HONO peak at 1263 cm^{-1} was identified after surface-adsorbed HNO_3 was exposed to NO. This peak corresponds to approximately 2×10^{14} molecules cm^{-3} of HONO, an amount that is significantly greater than what is observed as a trace impurity in the NO (Figure 2c). The small yields of HONO suggest that if the reaction of NO with HNO_3 is the source of HONO, removal of HONO by rapid secondary reactions must be occurring simultaneously in this system.

Although the NO also had small amounts of NO_2 and N_2O impurities, Figure 3 shows that there were no secondary reactions of these trace contaminants with the surface HNO_3. Thus, no new infrared bands were observed on addition of either NO_2 or N_2O to the cell containing adsorbed HNO_3, and there was no loss of adsorbed HNO_3 or the gaseous NO_2 and N_2O with time.

B. Possible Reaction Mechanisms. The experimental observations are consistent with the following heterogeneous reactions:

$$NO(g) + HNO_3(ads) \xleftrightarrow{surface} NO_2 + HONO \quad (5, -5)$$

$$HONO + HNO_3(ads) \xleftrightarrow{surface} 2\,NO_2 + H_2O \quad (6, -6)$$

$$2\,HONO \xleftrightarrow{surface} NO + NO_2 + H_2O \quad (7, -7)$$

Both reactions 5 plus 6 or 2 × reaction 5 plus reaction 7 give the net reaction 8:

$$NO + 2HNO_3 \xrightarrow{surface} 3NO_2 + H_2O \quad (8)$$

This net reaction is consistent, within experimental error, with the measured reaction stoichiometries shown in Table 1 for $\Delta HNO_3/\Delta NO = 1.9 \pm 0.3$, $\Delta NO_2/\Delta NO = 2.2 \pm 0.3$, $\Delta HNO_3/\Delta NO_2 = 0.9 \pm 0.2$, and $\Delta NO_2/(\Delta NO + \Delta HNO_3) = 0.8 \pm 0.1$ (2σ). Deviations from the expected stoichiometries involving NO_2 are consistent with underestimation of the yield of NO_2, because the gas and surface-adsorbed N_2O_4 have not been taken into account in calculating these ratios.[26]

The heterogeneous formation of NO_2 by reaction 5 has been suggested by several authors attempting to study the gas-phase reaction, i.e., reaction 3.[12−15] This reaction in the gas phase is approximately thermoneutral, $\Delta H° = -1.4$ kJ mol^{-1}, and it is common for such reactions to proceed more rapidly on surfaces.[19] Reaction 4, which is the gas-phase equivalent of reaction 6, is 39.2 kJ mol^{-1}endothermic, making the overall reaction 8 endothermic by 37.8 kJ mol^{-1} if all of the reactants

TABLE 1: Initial Reactant HNO_3 and NO and Measured Stoichiometry for Reactants and Product NO_2

run	HNO_3(ini)[a]	HNO_3(ss)[a]	ΔHNO_3[b]	NO(ini)[c]	NO(ss)[c]	ΔNO[d]	ΔNO_2[e]	$\Delta HNO_3/\Delta NO$	$\Delta HNO_3/\Delta NO_2$	$\Delta NO_2/\Delta NO$	ΔNO_2[f]/$\Delta NO + \Delta HNO_3$
1	1.1×10^{19}	3.4×10^{18}	7.6×10^{18}	4.8×10^{18}	1.1×10^{18}	3.7×10^{18}	9.0×10^{18}	2.0	0.85	2.4	0.79
2	9.9×10^{18}	3.2×10^{18}	6.7×10^{18}	5.1×10^{18}	1.3×10^{18}	3.7×10^{18}	7.7×10^{18}	1.8	0.87	2.1	0.74
3	9.4×10^{18}	3.0×10^{18}	6.4×10^{18}	5.3×10^{18}	1.4×10^{18}	3.9×10^{18}	8.5×10^{18}	1.7	0.76	2.2	0.83
4	9.3×10^{18}	1.0×10^{18}	8.3×10^{18}	1.5×10^{19}	1.1×10^{19}	4.1×10^{18}	8.1×10^{18}	2.0	1.0	2.0	0.66
5	2.6×10^{18}	1.3×10^{17}	2.5×10^{18}	5.1×10^{18}	3.8×10^{18}	1.3×10^{18}	3.0×10^{18}	1.9	0.82	2.3	0.79
6	2.4×10^{18}	1.1×10^{17}	2.3×10^{18}	5.1×10^{18}	3.9×10^{18}	1.2×10^{18}	2.6×10^{18}	1.9	0.88	2.1	0.74
							AVERAGE	1.9	0.9	2.2	0.8
							2σ	0.3	0.2	0.3	0.1

[a] Numbers of HNO_3 molecules on the porous glass plate before (ini) and after (ss) the reaction. [b] Numbers of HNO_3 molecules reacted. [c] Numbers of NO molecules in the reaction cell before (ini) and after (ss) the reaction. [d] Numbers of NO molecules reacted. [e] Numbers of NO_2 molecules produced by the reaction; this does not take into account small amounts of N_2O_4 in equilibrium with the NO. [f] This is the yield of NO_2 when the concentrations of NO_2 and HNO_3 have leveled off (e.g., Figure 5), divided by the sum of the of the losses of NO and HNO_3; to be consistent with the net reaction 8, the ratio should be 1.0.

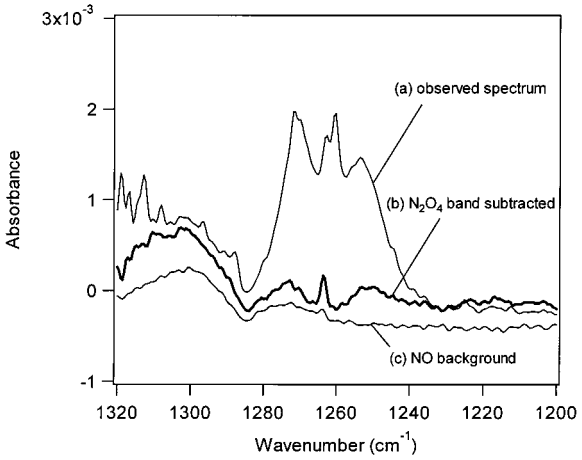

Figure 2. Gas-phase infrared spectra (a) after 120 min during the reaction of adsorbed HNO_3 (initially 9×10^{18} molecules) with 6.5×10^{16} molecules cm^{-3} NO, (b) after subtraction of the ν_{11} band of N_2O_4 from (a), showing the ν_3 band of gas phase *trans*-HONO whose intensity corresponds to a concentration of $\sim 2 \times 10^{14}$ molecules cm^{-3}, and (c) of NO alone; the small peak at 1263 cm^{-1} is due to trace impurity levels of HONO in the NO.

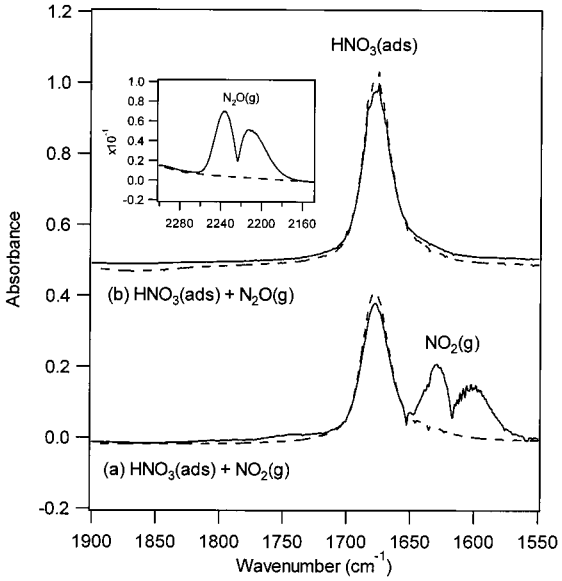

Figure 3. Infrared spectra of surface-adsorbed HNO_3 with some gaseous nitrogen oxides. (a) Dashed line: Adsorbed HNO_3 (9×10^{18} molecules) on porous glass. Solid line: after introduction of 6.5×10^{16} molecules cm^{-3} of NO_2. (b) Dashed line: adsorbed HNO_3 (1.1×10^{19} molecules) on porous glass. Solid line: after introduction of 6.5×10^{16} molecules cm^{-3} of N_2O.

and products were in the gas phase. However, the gas phase reactions 3 and 4 and their sum are all entropically favored, with $\Delta G^\circ = -11.8$ kJ mol^{-1} for the overall reaction.

To confirm the proposed mechanism, isotopically labeled ^{15}NO was used as a reactant in some experiments. At steady state, both isotopes $^{14}NO_2$ and $^{15}NO_2$ were identified as products by the $\nu_3+\nu_1$ band at 2907 and 2859 cm^{-1}, respectively. Both isotopomers were also confirmed from their parent peaks at $m/z = 46$ and 47 using mass spectrometry. This provides clear evidence that the nitrogen atom in surface adsorbed HNO_3 is involved in the reaction with NO. However, because of the fast interconversion between NO and NO_2,[27] which we also observed in separate experiments, it was not possible to trace the fate of ^{14}N and ^{15}N as a function of time; at steady-state, the ratio of $^{15}N/^{14}N$ of nitrogen compounds reached the same value as the ratio of ^{15}NO and $H^{14}NO_3$ initially present in the reaction cell.

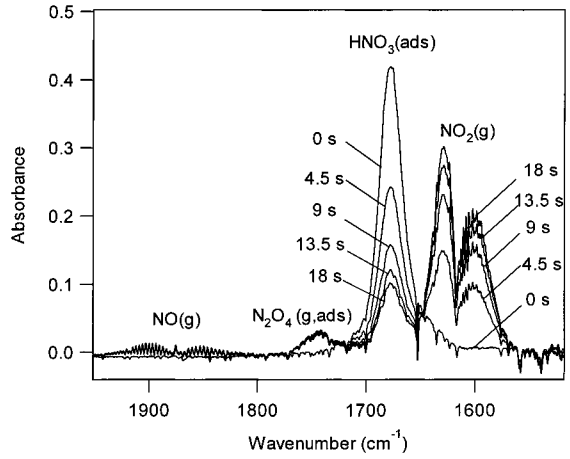

Figure 4. Infrared spectra of the combination of gas and adsorbed species after the reaction of surface adsorbed HNO_3 with gas-phase NO at various reaction times. The initial concentration of gas-phase NO was 6.7×10^{16} molecules cm^{-3} and the number of adsorbed HNO_3 determined by ion chromatography was 9×10^{18} molecules. The total pressure was 450 Torr in He carrier gas.

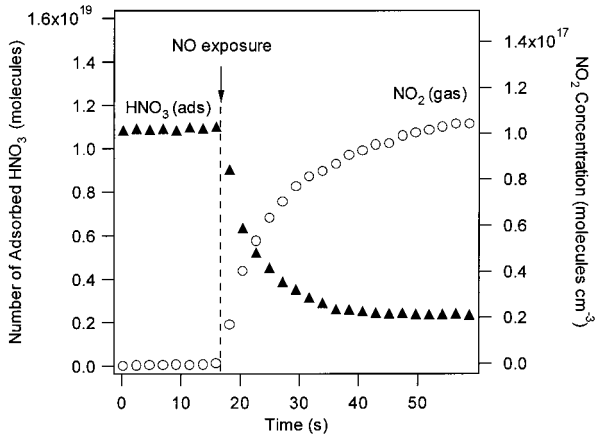

Figure 5. The time evolution of surface-adsorbed HNO_3 (1.1×10^{19} molecules) and product gaseous NO_2 measured using infrared bands at 1677 and 1620 cm^{-1}, respectively, when NO (6.1×10^{16} molecules cm^{-3}) was added to the cell in the presence of 450 Torr of He.

The presence of small amounts of HONO in the cell after the reaction of adsorbed HNO_3 with NO suggests that HONO is removed by a fast secondary reaction such as reactions 6 and/or 7. Reaction 6, whose reverse reaction (-6) is a well-known HONO formation pathway on surfaces,[28−35] is reported to proceed slowly in the gas phase[14−17] and is not important under our experimental conditions.[36] However, Wallington and Japar[17] report evidence that reaction 6 occurs heterogeneously as well. In the studies of Streit and co-workers,[15] the gas-phase reaction 4 of HNO_3 with HONO was found to be faster than reaction 3 of HNO_3 with NO. If the same is true for the analogous heterogeneous reactions 6 and 5, HONO may be removed rapidly by reaction 6 as it is formed.

HONO is also known to be in equilibrium with NO and NO_2 in the gas phase via reaction (7,-7).[28,29,37−42] While the gas-phase reaction cannot be important in our system,[43] a heterogeneous self-reaction of HONO on the porous glass surface cannot be ruled out. However, regardless of whether reaction 6 or 7 is more important, HONO can be consumed heterogeneously, leading to additional NO_2 formation.

As seen in Table 1 and Figure 5, in the presence of an excess stoichiometric amount of HNO_3 compared to NO (runs 1−3), HNO_3 levels off at nonzero levels at longer reaction times, with

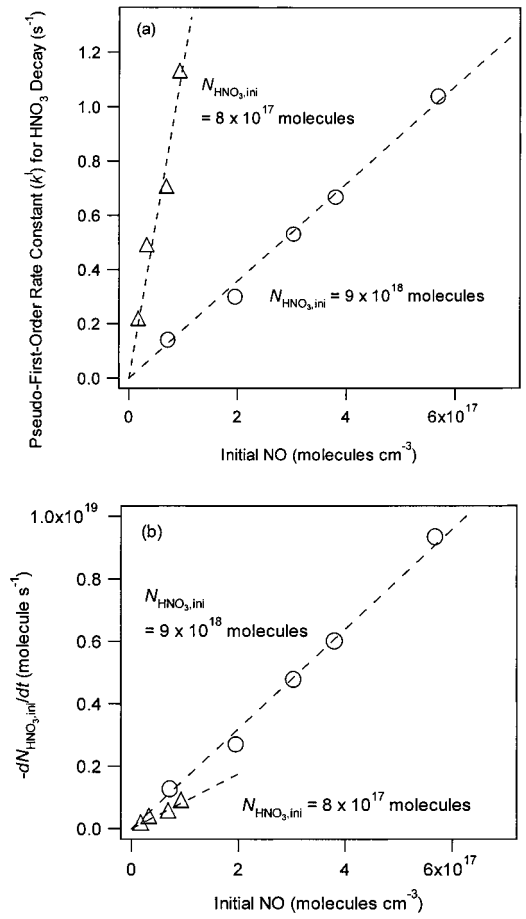

Figure 6. (a) The observed pseudo-first-order rate constants for HNO_3 decay on porous glass as a function of the initial NO concentration in the gas phase at two different initial amounts of adsorbed HNO_3. (b) Same as (a) but plotted in terms of the rate, $-dN_{HNO_3}/dt$ (molecules s^{-1}).

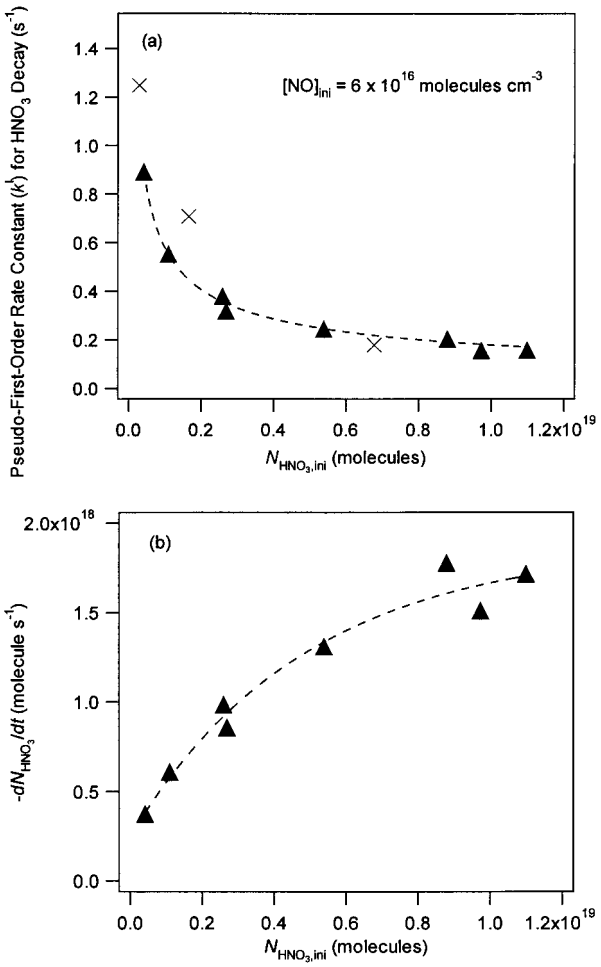

Figure 7. (a) Measured pseudo-first-order rate constants for HNO_3 decay as a function of initial adsorbed HNO_3 on the porous glass at a constant NO concentration of 6×10^{16} molecules cm^{-3} (total of 5×10^{18} molecules available for reaction in the cell). (▲) Porous glass pumped on but not heated. (×) Porous glass heated prior to reaction to remove some adsorbed water. (b) Same as (a) but plotted in terms of the rate $-dN_{HNO_3}/dt$.

approximately 25% of the initial NO remaining unreacted. This suggests that NO and HNO_3 may be regenerated in secondary reactions. In the case of NO, the bimolecular reaction 7 of HONO on surfaces generates NO, and the hydrolysis of NO_2 on surfaces is well-known to generate HNO_3.[1,28−35]

To explain their smog chamber results, Besemer and Nieboer[18] proposed that a reaction of NO with a species, likely HNO_3, on the walls of their reaction chamber produces HONO with the overall reaction being $2NO + HNO_3 \rightarrow 3HONO$. In their studies, the HONO was photolyzed as it was formed, so that secondary reactions such as reactions 6 and 7 were likely not important under their experimental conditions.

C. Kinetics of Reaction of HNO_3(ads) + NO(g) on Porous Glass. To examine how fast this reaction proceeds on silica surfaces, the decay of adsorbed HNO_3 and production of gaseous NO_2 were measured as a function of reaction time. A typical sequence of spectra is shown in Figure 4 and a typical time evolution of HNO_3 and gaseous NO_2 in Figure 5. The reaction reaches a steady-state in several seconds to several tens of seconds, depending on the initial concentrations of NO and adsorbed HNO_3. The pseudo-first-order rate constant for loss of HNO_3 (k^I) was found to be the same with or without He carrier gas in the cell.

Figure 6a shows the pseudo-first-order rate constants (k^I) for the initial decay of surface-adsorbed HNO_3 as a function of the initial NO concentration when the total amount of initial adsorbed HNO_3 is constant at either 0.8 or 9×10^{18} molecules, respectively. The values of k^I were derived from the initial slope of plot of ln N_{HNO_3} versus time. For initial HNO_3 of 9×10^{18} molecules, the decay to ~40% of the initial HNO_3 was followed; at initial HNO_3 of 8×10^{17} molecules, the decay was followed to ~20% of the initial value. The loss of NO was <20% under these conditions, except for one experiment at the highest HNO_3 and lowest NO, where the loss of NO was ~40%. The order of the reaction in NO can be obtained from $k^I = k^{II}[NO]^a$, where a is the reaction order in NO. The rate of HNO_3 decay (dN_{HNO_3}/dt, in molecule s^{-1}) is given by $k^I N_{HNO_3}$ and increases proportionally with NO (Figure 6b), i.e., $a = 1$.

The HNO_3 decay was also followed at a constant gas-phase NO concentration of 6×10^{16} molecules cm^{-3} with varying amounts (5×10^{17} molecules to 1.1×10^{19} molecules) of surface-adsorbed HNO_3. Figure 7a shows a negative dependence of the measured initial pseudo-first-order rate constants (k^I) for HNO_3 decay as a function of the initial number of adsorbed HNO_3 molecules, $N_{HNO_3,ini}$. In this case, the slopes of plots of ln N_{HNO_3} versus time over the first 2−4 s were used to obtain k^I. When expressed in the form $k^I = k^{II}(N_{HNO_3})^b$, a value of $b = -0.5$ gives the best fit to the data. To explore the possible effects of surface water, some experiments were carried out in which the outer portion of the cell containing the porous glass was heated to ~ 520 K while under vacuum for several hours. The integrated band intensity of the water peak at ~3500 cm^{-1} decreased by approximately a factor of 2. This did not

substantially alter the measured reaction stoichiometries. As seen in Figure 7a, the HNO_3 pseudo-first-order rate constants at the lower initial coverages increased somewhat, but in all cases by less than 50%. However, this does not rule out a role for surface water in the reaction, since the infrared spectrum of the porous glass indicated there were still substantial amounts of water available on the surface.

The initial rate of HNO_3 decay, i.e., $dN_{HNO_3}/dt = k^I N_{HNO_3,ini}$ in molecule s^{-1}, as a function of the initial adsorbed HNO_3, (Figure 7b) shows that the rate increases with $N_{HNO_3,ini}$, at low surface HNO_3, but drops off at higher surface coverages. This suggests that HNO_3 adsorbs to individual sites on the surface at low coverages, but completely covers the surface, forming multilayers at higher amounts of surface HNO_3. Given the porous nature of the surface, this multilayer formation may occur at least partially in the pores. At the lower coverages, the rate should depend linearly on the surface HNO_3 since increased amounts are available for reaction with gas phase NO. However, at the point of complete coverage or multilayer formation, only a constant amount of surface HNO_3 is available for reaction and the rate should become independent of the initial surface HNO_3, as appears to be the case (Figure 7b).

The fraction of available surface sites covered by HNO_3 initially under our experimental conditions can, in principle, be estimated from the measured BET surface area of 28.5 m^2. The adsorption site for HNO_3 may be surface −Si−OH groups. A fully hydroxylated surface has approximately 5×10^{14} Si−OH surface groups cm^{-2}.[21,44,45] If one HNO_3 is taken up per Si−OH group, a total of 1.4×10^{20} adsorption sites should be available. In this case, the HNO_3 coverages in these experiments would represent less than 10% of the surface adsorption sites. However, given the larger size of the HNO_3 molecule compared to N_2 used for the surface area measurements, and the possibility of water in the pores, all of the area inside the pores may not be available for uptake of HNO_3. It is therefore not unreasonable that high surface coverages and multilayers are obtained at the highest amounts of HNO_3 used in these studies.

D. Atmospheric Implications. The heterogeneous reaction of HNO_3 on silica surfaces with NO is clearly enhanced relative to the gas phase reaction. These experiments show that the rate increases linearly with NO. Although extrapolation to ambient air is uncertain, a rough estimate of the potential importance of this reaction can be assessed assuming the linear dependence on NO continues down to a typical ambient NO concentration of 10 ppbv in polluted areas, i.e., 2.5×10^{11} molecules cm^{-3}. From Figure 7a, the pseudo-first-order rate constant for HNO_3 decay at the lowest HNO_3 coverages is ~ 1 s^{-1} at an NO concentration of 6.5×10^{16} cm^{-3}. Linear extrapolation to an NO of 2.5×10^{11} molecules cm^{-3} gives $k^I = 4 \times 10^{-6}$ s^{-1} for the pseudo-first-order rate of HNO_3 decay on particles under these conditions. The importance of this heterogeneous reaction for the net loss of HNO_3 will depend on how much of the total HNO_3 in the atmosphere is adsorbed on particles relative to the amount in the gas phase, as well as the rates of the gas-phase reactions of HNO_3. Chemical losses for gas-phase HNO_3 include reaction with OH and photolysis, both daytime processes. Using the kinetics for the OH + HNO_3 reaction of Brown et al.,[46] the pseudo-first-order loss rate for HNO_3 with respect to reaction with OH at 1×10^6 radicals cm^{-3} (1 atm pressure at 298 K) is 1.6×10^{-7} s^{-1} (HNO_3 lifetime of ∼75 days). That for photolysis at a solar zenith angle of 50° at the earth surfaces is 3.4×10^{-7} s^{-1} (lifetime of 34 days), calculated using recommended actinic fluxes and absorption cross sections.[47] The lifetime with respect to deposition can be significantly shorter. However, under dry conditions above the boundary layer, deposition is less important.

Dentener et al.[48] have carried out global three-dimensional model studies of the uptake of HNO_3 and other gases on mineral aerosols and predict highly variable percentages of the total available HNO_3 which is on the mineral dust, varying from <20% to >90%. They assume that the major mechanism of uptake of gaseous HNO_3 is a neutralization reaction with particle components such as $CaCO_3$, which would leave nitrate, rather than adsorbed nitric acid, on the particles. However, if sufficient acidity were available to generate surface-adsorbed HNO_3, as might be the case in more polluted regions, the heterogeneous reaction with NO could be important. For instance, if 10% of the total HNO_3 were on the particles, the loss rates cited above imply that approximately half of the loss of HNO_3 in a volume of air containing 10 ppb NO could occur by the heterogeneous reaction. Furthermore, in urban areas, not only suspended particles but the surfaces of buildings, roads ,etc. may also adsorb HNO_3 and hence provide sites for the heterogeneous reaction with NO. Another possibility is uptake of HNO_3 into cirrus clouds and snow packs and its reaction with NO. Finally, although we have not directly observed the reaction, the reaction stoichiometry observed here suggests that the heterogeneous reaction 6 of gaseous HONO with surface adsorbed HNO_3 may also contribute to the reduction of HNO_3(ads) and to the removal of HONO in the atmosphere. This will depend on the rates of other processes for removal of HONO such as photolysis or advection away from the surface which are not important in our static experimental system.

In addition to regenerating photochemically active forms of NO_x from HNO_3, this heterogeneous reaction may be a significant source of HONO in urban atmospheres. For example, in a number of field studies where HONO as well as its precursors NO and NO_2 were measured, nighttime HONO concentrations were found to correlate best with the product $[NO][NO_2][H_2O]$ and possibly with a term for the concentration of particles available to enhance the heterogeneous reactions.[49−52] This correlation is not expected if the heterogeneous reaction −6 of NO_2 with water is the source of HONO, as commonly believed based on laboratory studies. As a result, the heterogeneous reaction of NO and NO_2 with water (or of N_2O_3 formed from NO and NO_2) on particles has often been suggested as a potential HONO source. The studies reported here suggest an alternate explanation for the correlation with NO, i.e., that it is the direct reaction of NO with surface-adsorbed HNO_3 that generates HONO. The importance of this source depends on whether the subsequent reactions of HONO with adsorbed HNO_3 is also fast under atmospheric conditions, as appears to be the case under our experimental conditions. It may also be that other condensed forms of nitric acid such as NH_4NO_3 undergo a similar reaction and could serve as a source of HONO in air. Further studies are underway to investigate these possibilities.

Conclusions

The heterogeneous reaction of surface adsorbed HNO_3 with gas-phase NO on silica surfaces has been observed at room temperature. Gaseous NO_2 was the major product. Small amounts of HONO were also observed. Yield measurements and isotope experiments using ^{15}NO support the hypothesis that HNO_3 can be converted to NO_2 via its reaction with NO, $HNO_3 + NO \rightarrow HONO + NO_2$, which is followed by $HONO + HNO_3 \rightarrow 2NO_2 + H_2O$ and/or $2 \times (HNO_3 + NO \rightarrow HONO + NO_2)$ followed by $2HONO \rightarrow NO + NO_2 + H_2O$, both leading to

the net reaction $2\ HNO_3 + NO \rightarrow 3NO_2 + H_2O$. Extrapolation to atmospheric conditions suggests that this reaction could be a significant HNO_3 reduction process in the atmosphere and contribute to the lower than the model-predicted values in the ratio of HNO_3 to NO_x measured in the troposphere[2] and perhaps to the high $[NO_x]/[HNO_3]$ ratio observed in snow packs.[7,8]

Acknowledgment. This work was supported by the California Air Resources Board (Contract No. 97-311) and the Research Fellowships of the Japan Society for the Promotion of Science for Young Scientists. We are also grateful to Dr. M. T. Kleinman for assistance with the ion chromatography, Professor K. Shea, D. Batra, and K. R. Muroya for assistance with the BET surface area measurements, M. E. Gebel for mass spectrometry, and Dr. J. N. Pitts, Jr., Professor J. C. Hemminger, and Dr. William S. Barney for helpful discussions.

References and Notes

(1) Finlayson-Pitts, B. J.; Pitts, J. N. *Chemistry of the Upper and Lower Atmosphere: Theory, Experiments and Applications*; Academic Press: San Diego, 2000 and references therein.

(2) Chatfield, R. B. *Geophys. Res. Lett.* **1994**, *21*, 2705−2708.

(3) Rogaski, C. A.; Golden, D. M.; Williams, L. R. *Geophys. Res. Lett.* **1997**, *24*, 381−384.

(4) Choi, W.; Leu, M. T. *J. Phys. Chem. A.* **1998**, *102*, 7618−7630.

(5) Hauglustaine, D. A.; Ridley, B. A.; Solomon, S.; Hess, P. G.; Madronich, S. *Geophys. Res. Lett.* **1996**, *23*, 2609−2612.

(6) Lary, D. J.; Lee, A. M.; Toumi, R.; Newchurch, M. J.; Pirre, M.; Renard, J. B. *J. Geophys. Res.* **1997**, *102*, 3671−3682.

(7) Honrath, R. E.; Peterson, M. C.; Guo, S.; Dibb, J. E.; Shepson, P. B.; Campbell, B. *Geophys. Res. Lett.* **1999**, *26*, 695−698.

(8) Jones, A. E.; Weller, R.; Wolff, E. W.; Jacobi, H. W. *Geophys. Res. Lett.* **2000**, *27*, 345−348.

(9) Johnson, E. R. *The Radiation-Induced Decomposition of Inorganic Molecular Ions*; Gordon and Breach: New York, 1970.

(10) Wagner, I.; Strehlow, H.; Busse, G. *Z. Phys. Chem.* **1980**, *123*, 1−33.

(11) Vogt, R.; Finlayson-Pitts, B. J. *J. Phys. Chem.* **1995**, *99*, 17269−17272.

(12) Smith, J. H. *J. Am. Chem. Soc.* **1947**, *69*, 1741−1747.

(13) Jaffe, S.; Ford, H. W. *J. Phys. Chem.* **1967**, *71*, 1832−1836.

(14) Kaiser, E. W.; Wu, C. H. *J. Phys. Chem.* **1977a**, *81*, 187−190.

(15) Streit, G. E.; Wells, J. S.; Fehsenfeld, F. C.; Howard, C. J. *J. Chem. Phys.* **1979**, *70*, 3439−3443.

(16) England, C.; Corcoran, W. H. *Ind. Eng. Chem. Fundam.* **1975**, *14*, 55−63.

(17) Wallington, T. J.; Japar, S. M. *J. Atmos. Chem.* **1989**, *9*, 399−409.

(18) Besemer, A. C.; Nieboer, H. *Atmos. Environ.* **1985**, *19*, 507−513.

(19) Fairbrother, D. H.; Sullivan, D. J. D.; Johnston, H. S. *J. Phys. Chem. A* **1997**, *101*, 7350−7358.

(20) Barney, W. S.; Finlayson-Pitts, B. J. *J. Phys. Chem. A* **2000**, *104*, 171−175.

(21) Kiselev, A. V.; Lygin, V. I. *Infrared Spectra of Surface Compounds*; Wiley: New York, 1975.

(22) Barney, W. S.; Wingen, L. M.; Lakin, M. J.; Brauers, T.; Stutz, J.; Finlayson-Pitts, B. J. *J. Phys. Chem. A* **2000**, *104*, 1692−1699.

(23) Goodman, A. L.; Underwood, G. M.; Grassian, V. H. *J. Phys. Chem. A.* **1999**, *103*, 7217−7223.

(24) Querry, M. R.; Tyler, I. L. *J. Chem. Phys.* **1980**, *72*, 2495−2499.

(25) Biermann, U. M.; Luo, B. P.; Peter, T. *J. Phys. Chem. A.* **2000**, *104*, 783−793.

(26) This is supported by separate studies using a long path (40 m) gas cell whose walls were doped with HNO_3. NO in N_2 at 50% relative humidity was then added. The stoichiometry $\Delta NO_2/\Delta NO$ was measured to be 3.5 ± 0.5 (2σ) at NO concentrations down to 26 ppm where N_2O_4 formation is not important, unlike the present studies at higher concentrations where N_2O_4 is observed (Saliba, N.; Mochida, M.; Finlayson-Pitts, B. J. *Geophys. Res. Lett.* In press.).

(27) Sharma, H. D.; Jervis, R. E.; Wong., K. Y. *J. Phys. Chem.* **1979**, *74*, 923−933.

(28) Sakamaki, F.; Hatakeyama, S.; Akimoto, H. *Int. J. Chem. Kinet.* **1983**, *15*, 1013−1029.

(29) Pitts, J.; J. N.; Sanhueza, E.; Atkinson, R.; Carter, W. P. L.; Winer, A. M.; Harris, G. W.; Plum, C. N. *Int. J. Chem. Kinet.* **1984a**, *16*, 919−939.

(30) Svensson, R.; Ljungstrom, E.; Lindqvist, O. *Atmos. Environ.* **1987**, *21*, 1529−1539.

(31) Jenkin, M. E.; Cox, R. A.; Williams, D. J. *Atmos. Environ.* **1988**, *22*, 487−498.

(32) Febo, A.; Perrino, C. *Atmos. Environ.* **1991**, *25A*, 1055−1061.

(33) Bambauer, A.; Brantner, B.; Paige, M.; Novakov, T. *Atmos. Environ.* **1994**, *28*, 3225−3232.

(34) Mertes, S.; Wahner, A. *J. Phys. Chem.* **1995**, *99*, 14000−14006.

(35) Kleffmann, J.; Becker, K. H.; Wiesen, P. *Atmos. Environ.* **1998a**, *32*, 2721−2729.

(36) At a gas-phase HNO_3 concentration of $\leq(1-2) \times 10^{15}$ molecules cm^{-3} and a HONO concentration of 1×10^{16} molecules cm^{-3} (2 orders of magnitude larger than observed) and using the upper limit for the gas-phase rate constant of $k_4 < 7 \times 10^{-19}$ cm^3 $molecule^{-1}$ s^{-1} reported by Wallington and Japar,[17] only 6×10^{14} molecules cm^{-3} of NO_2, corresponding to a total of 4×10^{16} NO_2 in the cell, would be generated in 20 s, about 2 orders of magnitudes less than observed (Table 1).

(37) Wayne, L. G.; Yost, D. M. *J. Chem. Phys.* **1951**, *19*, 41−47.

(38) Graham, R. F.; Tyler, B. J. *J. Chem. Soc., Faraday Trans. 1* **1972**, *68*, 683−688.

(39) Chan, W. H.; Nordstrom, R. J.; Calvert, J. G.; Shaw, J. H. *Chem. Phys. Lett.* **1976a**, *37*, 441−446.

(40) Chan, W. H.; Nordstrom, R. J.; Calvert, J. G.; Shaw, J. H. *Environ. Sci. Technol.* **1976b**, *10*, 674−682.

(41) Cox, R. A.; Derwent, R. G. *J. Photochem.* **1976/77**, *6*, 23−34.

(42) Kaiser, E. W.; Wu, C. H. *J. Phys. Chem.* **1977b**, *81*, 1701−1706.

(43) Kaiser and Wu[42] reported an upper limit for the gas-phase rate constant of $k_7 < 1 \times 10^{-20}$ cm^3 $molecule^{-1}$ s^{-1}. At a HONO concentration of 10^{16} molecules cm^{-3}, only $\sim 10^{15}$ molecules of NO_2 would be generated in 20 s, much less than observed (Table 1).

(44) Zhuravlev, L. T. *Colloids Surf.* **1993**, *74*, 71−90.

(45) Sneh, O.; Cameron, M. A.; George, S. M. *Surface Science* **1996**, *364*, 61−78.

(46) Brown, S. S.; Talukdar, R. K.; Ravishankara, A. R. *J. Phys. Chem. A.* **1999**, *103*, 3031−3037.

(47) DeMore, W. B.; Sander, S. P.; Golden., D. M.; Hampson, R. F.; Kurylo, M. J.; Howard, C. J.; Ravishankara, A. R.; Kolb, C. E.; Molina, M. J. Chemical Kinetics and Photochemical Data for Use in Stratospheric Modeling, Evaluation No. 12. In *JPL Publications*; Jet Propulsion Laboratory: Pasadena, 1997; Vol. 97-4.

(48) Dentener, F. J.; Carmichael, G. R.; Zhang, Y.; Lelieveld, J.;.Crutzen, P. J. *J. Geophys. Res.* **1996**, *101*, 22, 869−22, 889.

(49) Sjodin, A.; Ferm, M. *Atmos. Environ.* **1985**, *19*, 985−992.

(50) Notholt, J.; Hjorth, J.; Raes, F. *Atmos. Environ.* **1992**, *26A*, 211−217.

(51) Winer, A. M.; Biermann, H. W. *Rev. Chem. Intermed.* **1994**, *20*, 423−445.

(52) Calvert, J. G.; Yarwood, G.; Dunker, A. M. *Res. Chem. Intermed.* **1994**, *20*, 463−502.